ESync: Energy Synchronized Mobile Charging in Rechargeable Wireless Sensor Networks

Lingkun Fu, *Member, IEEE*, Liang He, *Member, IEEE*, Peng Cheng, *Member, IEEE*, Yu Gu, *Member, IEEE*, Jianping Pan, *Senior Member, IEEE*, and Jiming Chen, *Senior Member, IEEE*

***Abstract*—Recent years have witnessed many new promising technologies to power wireless sensor networks, which motivate some fundamental topics to be revisited. Different from energy harvesting, which generates dynamic energy supply, the mobile charger is able to provide a stable and reliable energy supply for sensor nodes and, thus, enables sustainable system operations. While previous mobile charging protocols focus on either the charger travel distance or the charging delay of sensor nodes, in this work, we propose a novel *energy synchronized mobile charging (ESync)* protocol, which simultaneously reduces both of them. Observing the limitation of *traveling salesman problem* (TSP)-based solutions, when the nodes' energy consumption is diverse, we construct a set of nested TSP tours based on their energy consumption, and only nodes with low remaining energy are involved in each charging round. Furthermore, we propose the concept of energy synchronization to synchronize the charging request sequence of nodes with their sequence on the TSP tours. Experimentation and simulation demonstrate that *ESync* can reduce charger travel distance and nodes' charging delay by about 30% and 40%, respectively.**

***Index Terms*—Energy synchronization, mobile charger, on-demand energy replenishment, wireless sensor networks.**

I. Introduction

As most existing sensor networks are powered by batteries, their lifetime is limited by battery capacity. Hence, energy efficiency is essential because the energy resources of sensor nodes are limited and can be easily exhausted, and how to optimally distribute energy in wireless sensor networks has become an emerging issue [2]–[4], [55]. One key issue in wireless sensor networks is the energy provisioning problem, i.e., how to distribute energy in an optimal manner to power a network [5], [6]. The recent research breakthrough in wireless energy transfer technology developed by Kurs *et al.* [7] provides a promising technology to power these sensor nodes. To address the energy constraints of sensor nodes [8]–[13], the concepts and implementations of adopting mobile chargers to replenish the nodes' energy supply in rechargeable sensor networks have attracted a lot of attention in the research community recently [14]–[20]. Different from traditional energy harvesting sensor networks [21]–[26], where the harvested energy is dynamic in both the spatial and temporal dimensions, the mobility-assisted energy replenishment provides stable and reliable energy supply for sensor nodes and, thus, enables truly sustainable operations of sensor networks [27]–[30].

In a practical scenario, due to the limited charger mobility, the scheduling of charging tasks for sensor nodes in the network plays a critical role in achieving high charging efficiency. The *traveling salesman problem* (TSP)-based charging protocols are a family of classic solutions to the mobile charging problem [17], with which in general, the mobile charger *periodically* carries out the charging process following a *preoptimized* tour. As a result, the charging of nodes can be accomplished with a short charger travel distance and, thus, a short time duration.

However, the limitation of TSP-based solutions is that when the nodes' energy consumption is diverse, it may lead to the unnecessary visits of energy-sufficient nodes. This not only increases the charger travel distance when performing the charging tasks of sensor nodes but also prolongs the waiting time before the energy-hungry nodes can be charged. To address this issue, in this paper, we investigate the on-demand mobile charging scenario where nodes are charged only when necessary. Specifically, sensor nodes send out charging requests to the mobile charger when their energy levels are low, and the charger replenishes their energy supply according to those received requests. We aim to design a novel mobile charging protocol that is able to leverage on the advantages of existing designs while minimizing the impact of their limitations.

The most significant feature in our design is *synchronizing the energy supply of sensor nodes based on a set of nested TSP tours*. Upon achieving such energy synchronization, we can realize the ideal mobile charging paradigm that the charger can simply travel according to the TSP tours to reduce its travel distance, and whenever a sensor node runs short of energy, the

Manuscript received May 14, 2015; revised August 16, 2015; accepted September 13, 2015. Date of publication September 24, 2015; date of current version September 15, 2016. This work was supported in part by the National Natural Science Foundation of China under Grant U1401253 and Grant 61473251; by the National Program for Special Support of Top Notch Young Professionals; by ZJNSF under Grant LY14F030016; by the Key Laboratory of Computer Network and Information Integration (Southeast University), Ministry of Education of China, under Grant K93-9-2015-02B; and by the Natural Sciences and Engineering Research Council of Canada. This paper was presented in part at the ACM International Symposium on Mobile Ad Hoc Networking and Computing, Philadelphia, PA, USA, August 11–14, 2014. The review of this paper was coordinated by Prof. G. Mao.

L. Fu, P. Cheng, and J. Chen are with the State Key Laboratory of Industrial Control Technology, Zhejiang University, Hangzhou 310027, China (e-mail: lkfu@iipc.zju.edu.cn; pcheng@iipc.zju.edu.cn; jmchen@iipc.zju.edu.cn).

L. He is with the University of Michigan, Ann Arbor, MI 48109 USA, and also with the Key Laboratory of Computer Network and Information Integration, Southeast University, Ministry of Education, Beijing 100044, China (e-mail: lianghe@umich.edu).

Y. Gu is with Watson Health Cloud, IBM Watson Health, Cambridge, MA 02142 USA (e-mail: yugu@us.ibm.com).

J. Pan is with the Department of Computer Science, University of Victoria, Victoria, BC V8P 5C2, Canada (e-mail: pan@uvic.ca).

Color versions of one or more of the figures in this paper are available online at http://ieeexplore.ieee.org.

Digital Object Identifier 10.1109/TVT.2015.2481920

charger will *happen to* be traveling toward it. Our major intellectual contributions in this paper are fourfold.

- To the best of our knowledge, our work is the first to jointly improve the charging process for both sensor nodes and the mobile charger. Most existing works choose only one of the two given aspects as the design objective.
- At the macro level of the mobile charging process, to leverage the advantage of the TSP-based solutions while minimizing the impact of their limitations when node energy consumption is highly diverse, we construct a set of nested TSP tours based on the energy consumption rates of sensor nodes. Then, for each round of the charging process, a novel tour selection algorithm is designed to only involve the energy-hungry nodes into the charging schedule during that round.
- At the micro level, focusing on the charging schedule during individual rounds, observing that the nodes' charging request sequence may significantly affect the charging performance, we propose the concept of *energy synchronization* among nodes to proactively match the nodes' charging request sequence to the selected TSP tour in each charging round, which is achieved by carefully selecting the node to be charged next and controlling the amount of energy charged to individual nodes. As a result, both the charger travel distance and the charging delay of sensor nodes are reduced.
- We evaluate the performance of *ESync* through both experiment and simulations, and the results demonstrate that *ESync* can reduce the charger travel distance and charging latency by 30% and 40%, respectively.

This paper is organized as follows. Section II briefly reviews the literature. We introduce the problem statement in Section III. Our design on the nested TSP tours is presented in Section IV, and the design on the energy synchronization among nodes is introduced in Section V. More insights into *ESync* are presented in Section VI. Sections VII and VIII present the evaluation results obtained through both experiment and simulations, and we conclude in Section IX.

II. Related Work

The mobility-assisted energy replenishment provides stable and reliable energy supply for sensor nodes and has attracted increasing attention from the research community recently [14]–[20]. The mobile charging process can be evaluated from the perspective of the charger and sensor nodes, respectively. For the charger, the optimization objective is to minimize its travel distance when performing the charging tasks [16], [28]. The most intuitive approach is to periodically charge nodes along an optimal TSP tour constructed based on network deployment [17]. The problems of mobile energy replenishment and data gathering are jointly optimized in [18].

Several other designs tackle the mobile charging problem from the perspective of individual sensor nodes [14], [15]. A scheme jointly exploring the routing and charging of individual nodes is proposed in [14], which proactively guides the routing activities in the network and delivers energy to where it is needed. A greedy charging algorithm that always charges the node with the shortest remaining lifetime to its full capacity is proposed in [15] and is further improved by incorporating the remaining energy levels of other nodes when determining which node to charge next and how much energy to charge to. The design is validated based on a proof-of-concept prototype of a wireless charging system for sensor networks. Another way to greedily perform the charging tasks is to always select the nearest requesting node to charge, i.e., the Nearest-Job-Next discipline. The performance of Nearest-Job-Next is analytically evaluated in [31] and [32]. Although asymptotically promising, the worst-case performance of Nearest-Job-Next is difficult to guarantee.

With the concept of energy synchronization among nodes based on a set of nested TSP tours, we propose a novel mobile charging protocol that leverages on the advantages of both the existing designs while minimizing the impact of their drawbacks. Our design reduces the charger travel distance by scheduling based on the nested TSP tours and reduces the charging delay of sensor nodes with the concept of energy synchronization within each round of selected tours.

III. Preliminaries

A. Problem Statement

With the advancement of the energy transferring technologies, the time to replenish the energy supply of sensor nodes has been dramatically reduced [28], [33]. Zhu *et al.* have implemented an energy sharing system with capacitor-array-powered sensor nodes [25], in which the energy supply in the network is transferred from energy-sufficient nodes to energy-hungry nodes. From the empirical results reported in [24], the time to charge a 10-F capacitor from empty to a voltage of 2.5 V is on the order of 10 s normally. This greatly shortened charging time indicates that adopting mobile chargers to replenish the nodes' energy supply is a promising direction for stable and sustainable network operations.

In this paper, we investigate the on-demand mobile charging problem in rechargeable sensor networks, where a mobile energy charger travels within the deployment field and replenishes the energy supply of nodes. The mobile charger is controllable in both its travel trajectory and the amount of energy charged to individual sensor nodes.

Various technologies are available to transfer energy from the charger to sensor nodes, e.g., the contact-based and the short-distance charging technologies such as *inductive charging* [34]. It is reported in [35] that the 2-D waveguide power transmission technology can achieve an energy efficiency of 87.7%. To facilitate the practical implementation of the contact-based charging, a sensor-based docking mechanism was designed and implemented in [36]. The contact-based charging technology is also adopted in off-the-shelf products such as iRobot Roomba [37] and Nokia wireless charging plate for smartphones [38], and the short-distance charging technology has been implemented in the online electric vehicle system by KAIST [39]. Based on these various feasible charging technologies, in this paper, we focus on a general mobile charging scenario without requiring

any specific way to transfer energy from the charger to sensor nodes.

When the remaining energy levels of sensor nodes are low, the nodes initiate charging requests to the mobile charger either by communications (potentially in multiple hops) between themselves and the charger [40], [41] or with the assistance of a sink [14], [15].[1] Our objective is to design an efficient mobile charging protocol for the charger to effectively serve the received charging requests. Here, by *serving* a charging request, we mean the charger travels to the requesting sensor node and replenishes its energy supply to the desired level. The mobile charging process can be evaluated from two aspects.

- **Charging Delay** For the requesting sensor nodes, the charging process is evaluated based on their *charging delay*, which is defined as the period from the time they send out their charging requests to the time their energy is replenished by the charger, which consists of two components: the travel time of the charger to reach the node and the time to actually charge the node. A shorter charging delay implies higher charging efficiency.
- **Charger Travel Distance** For the mobile charger, the charging efficiency is evaluated in terms of its *travel distance* to carry out the charging tasks of nodes. A shorter travel distance indicates higher charging efficiency.

Most existing works choose only one of the two given aspects as the design objective. For example, reducing the charging latency of sensor nodes is emphasized in [14] and [15], whereas the charging process is optimized by shortening the charger travel distance in [17]. To the best of our knowledge, our work is the first attempt to jointly tackle these two objectives.

B. State of the Art and Limitations

The TSP-based solutions are a classic family of the designs on the mobile charging problem [17]. In general, with the TSP-based solutions, the mobile charger *periodically* travels along a preoptimized TSP tour to replenish the energy supply of nodes in each round of the charging process, and thus, the charger travel distance in replenishing the energy of all nodes is minimized. However, to take advantage of the preoptimized TSP tour in the on-demand mobile charging scenario, there are two facts that would significantly degrade the charging performance.

1) Diversity in Node Energy Consumption: The efficiency of the TSP-based solutions degrades when the nodes' energy consumption rates are highly diverse, which is unfortunately true in most cases for multihop sensor networks [42]. The high-energy-consumption diversity may cause highly diverse nodes' remaining energy levels, and as a result, traveling along the preoptimized tour leads to the unnecessary visits of energy-sufficient nodes. This not only increases the charger travel distance but also prolongs the charging delay of energy-hungry nodes.

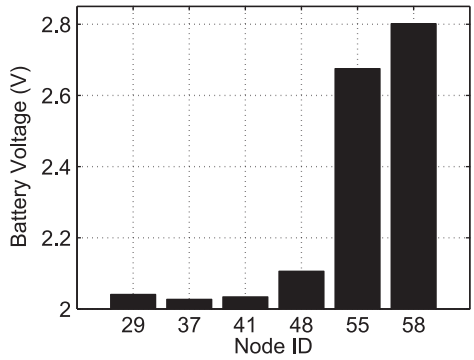

Fig. 1. Diverse nodes' remaining energy (original data are provided in [43]).

To clearly demonstrate the potentially unnecessary visits of energy-rich nodes, Fig. 1 presents the voltage readings of six sensors at a specific time in a data trace provided by Intel Berkeley Research lab, which is collected with the granularity of 1 s between February 28, 2004 and April 5, 2004 [43]. We can observe obvious voltage diversity among the nodes. In this case, if the charger carries out the charging process based on the TSP tour constructed according to these six nodes, it would arrive at node-55 and node-58, only to find out that they have little demand for energy replenishment.

2) Sequence of Node Charging Requests: Furthermore, in the on-demand charging scenario, even if nodes have similar energy consumption, indicating that they may all need to be charged in a given round, their charging request sequence plays a critical role in determining the performance of the periodic charging process, which must be considered if we want to utilize the advantage of the TSP-based solutions in minimizing the charger travel distance. Fig. 3 demonstrates an example of how the charging request sequence affects the charging performance. Consider the network shown on the upper-right corner of the figure, where the charger periodically carries out the charging tasks according to the optimal TSP tour shown with the dashed lines. If node E requests charging when the charger has just charged A, which means that the charger has already passed E in this round, the charger would first charge nodes B, C, and D if necessary. This way, the energy of E will not be replenished until the charger reaches it in the next round, which leads to a large charging delay of E. The fundamental reason for E's long charging delay in the given example is that the charging request sequence (i.e., A requests earlier than E) mismatches with the node sequence on the optimal TSP tour (i.e., A is after E along the tour). To examine whether the mismatching between the two sequences exists in practice, we simulate a small environment monitoring sensor network consisting of 20 sensor nodes with similar energy consumption. We construct a near-optimal TSP tour based on the nodes' deployment with the open-source TSP solver *Concorde* [44] and index nodes according to their sequence along the tour. We record the charging request sequence of nodes, and the first 100 requests are shown in Fig. 2, where the x-axis is the requesting sequence, and the y-axis is the index of the corresponding requesting node. We can see that the index of requesting nodes

[1]A remaining energy level threshold can be adopted for sensor nodes to initiate their charging requests. For ease of description, we assume a threshold of 0% in this paper. Furthermore, as both the time for the charger to travel to the requesting node and the time to replenish the nodes' energy supply are normally much longer than the communication delay, we assume a negligible time to deliver charging requests from nodes to the charger, which is similar to [42].

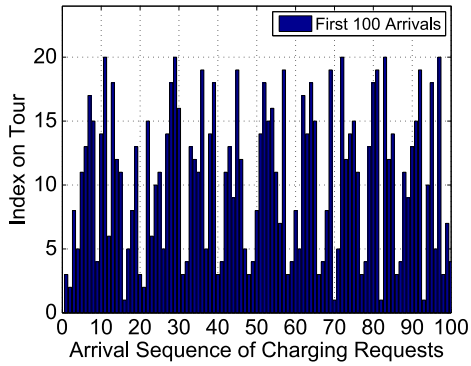

Fig. 2. Request sequence mismatches node sequence along the tour.

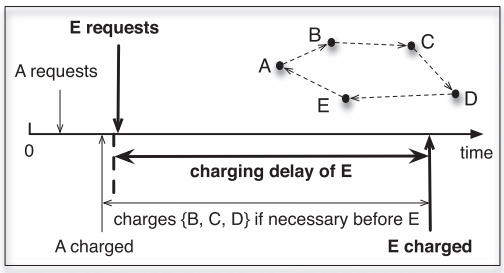

Fig. 3. Request sequence affects the charging performance significantly. The charging delay of E is long if E requests charging when the charger has already passed it in the current charging round.

is quite random with regard to the nodes' requesting sequence, which would lead to the undesired case shown in Fig. 3.

It is possible to avoid the undesired case shown in Fig. 3 by removing the periodic property from the charging process, e.g., performing charging tasks according to the classic Nearest-Job-Next discipline [31]. However, removing the periodic property may lead to the *zig-zag* travel of the charger and cause an unfairness issue among sensor nodes. Our evaluation results show that the proposed design in this work outperforms Nearest-Job-Next by about 30%–40%, as will be explained in Sections VII and VIII.

C. Design Overview

In this paper, focusing on the scenario where the energy consumption rates are diverse among sensor nodes, we propose the *energy synchronized mobile charging (ESync)* protocol, which addresses the two given limitations by first *constructing a set of nested TSP tours* and then *synchronizing the nodes' energy according to the tours*. The motivation of the nested TSP tours is to only involve nodes with low remaining energy levels in each charging round to reduce the charger travel distance. The motivation for the energy synchronization among nodes is to proactively adjust the nodes' charging request sequence to synchronize it with the TSP tour selected in each round and, thus, reduce the charging delay of sensor nodes.

IV. Construction of Nested Traveling Salesman Problem Tours

The limitation of the TSP-based solutions with diverse node energy consumption inspires us with the following question: *Instead of scheduling the charging tasks based on a single tour, is it possible to preoptimize a set of tours to guide the charging process in each round, such that only energy-hungry nodes are involved in each round?* Our approach is to cluster nodes according to their energy consumption rates, and then based on these clusters, we construct multiple TSP tours in a *nested* manner. We further present a corresponding tour selection algorithm to guide the charging process in each round.

A. Power-α Clustering

Before introducing the design of our clustering algorithm, we first use a simplified example as shown in Fig. 4 to present our idea. The energy consumption rates of nodes represented by the squares are twice those of the triangle nodes and four times those of the circle nodes. Denote the lifetime of square nodes when fully charged by T. Consequently, the triangle and circle nodes have a $2T$ and $4T$ lifetime when fully charged, respectively.[2]

If we take these three classes of nodes as three clusters, then when the square nodes deplete their energy after an operation time of T, the charger only needs to charge the square cluster as both the triangle and circle nodes still have sufficient energy supply [see Fig. 4(1)]. The nodes' remaining energy levels after the charging of the square nodes are shown in Fig. 4(2).[3] After another operation time of T, both the square and triangle nodes deplete their energy, and this time, the charger needs to charge the two corresponding clusters, as shown in Fig. 4(3). When an operation time of $4T$ is passed, the charger needs to replenish the energy supply of all nodes, as shown in Fig. 4(7), and the process repeats afterward.

In this example, the node clusters can accurately separate the energy-hungry nodes from the energy-rich nodes in each charging round, and thus, the charger only needs to consider the node clusters, instead of individual nodes, to carry out the charging process. The fundamental property that leads to this effect is that nodes in the same cluster have similar energy consumption. Based on this observation, we propose a novel *power-α* clustering algorithm to group nodes according to their energy consumption.

Assuming all nodes are initially fully charged, we begin our design from the time that at least one charging request has been received from each node. This ensures that the charger has certain knowledge on the energy consumption conditions of all nodes, based on which the estimation on their energy consumption rates is feasible [45]. The charger can adopt any existing charging protocols before this time [14], [31], [32]. Note that the perfect estimation on node energy consumption rates is extremely challenging. The energy consumption of nodes varies in both the spatial (i.e., different nodes may have different consumption rates) and temporal dimensions (i.e., the energy consumption rate of the same node may vary over time). Our

[2]To highlight the motivation of our design, the nodes' energy consumption rates in this example are intentionally set to diverse. However, our design is also applicable to scenarios where nodes have similar energy consumption.

[3]The time to finish the charging of these nodes is assumed to be negligible for ease of demonstration. However, we do incorporate it into our design, as will be shown later in Section V.

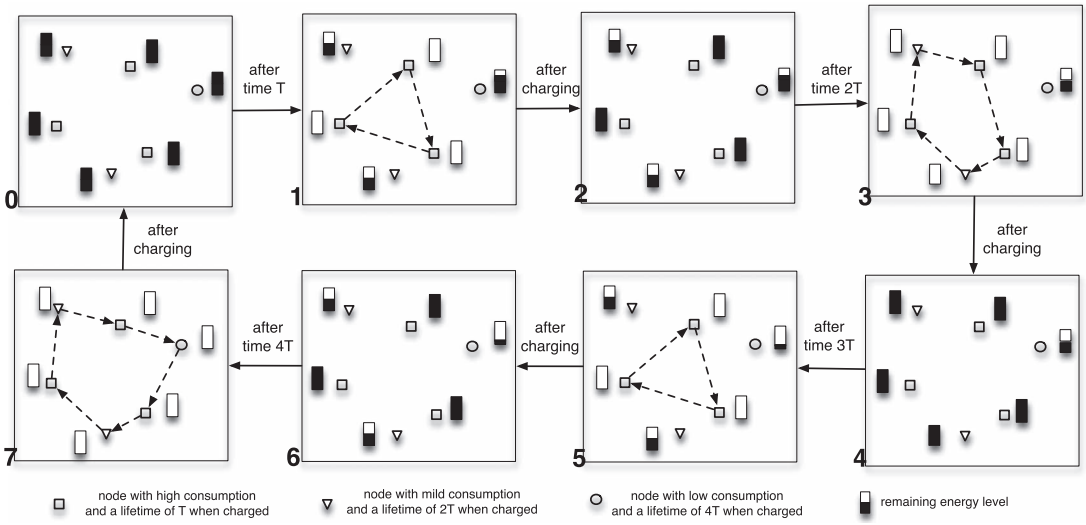

Fig. 4. Clustering nodes according to their energy consumption rates. A set of nested TSP tours is then constructed. One of these TSP tours is selected to guide the charging tasks in each round.

design does not require the perfect estimation of node energy consumption rates, and we will further discuss and investigate the charging performance under varying estimation errors in Sections VII and VIII. Through our experiment and simulation, we observe that our design can tolerate up to 30% estimation errors on the energy consumption rates of sensor nodes, which can be easily guaranteed by the state-of-the-art power monitoring solutions [46], [47]. Furthermore, in recent works [48], authors have proposed an efficient approach to collect the energy information of sensor nodes, which facilitates the mobile charger to be more accurate about the energy consumption of nodes. In addition, the mechanisms proposed to handle emergencies when nodes drain energy faster than anticipated can also be incorporated to *ESync* as mitigation to highly variable energy consumption rates of nodes.

Denote $r_{\max}$ and $r_{\min}$ as the maximal and minimal energy consumption rates of sensor nodes in the network, respectively. We construct a total number of m intervals and

$$m = \left\lceil \log_\alpha \left(\frac{r_{\max}}{r_{\min}} \right) \right\rceil^+ \tag{1}$$

where $\lceil x \rceil^+$ returns the first integer that is larger than x,[4] and α is an integer design parameter that is larger than 1. With the ascending order of energy consumption rates, these m intervals are

$$\left[r_{\min}, \frac{r_{\max}}{\alpha^{m-1}} \right], \left(\frac{r_{\max}}{\alpha^{m-1}}, \frac{r_{\max}}{\alpha^{m-2}} \right], \ldots, \left(\frac{r_{\max}}{\alpha^{1}}, r_{\max} \right]. \tag{2}$$

Note that the length of each interval exponentially increases with α. For each node s, it is clustered into the ith cluster if its energy consumption rate $r(s)$ falls into the ith interval. For example, if $r_{\max} = 6$, $r_{\min} = 1$, and $\alpha = 2$, then $m = \lceil \log_2(6/1) \rceil^+ = 3$ intervals are constructed. The three intervals are [1, 1.5], (1.5, 3], and (3, 6], respectively. For clarity, we refer to the interval with the highest consumption rate (i.e., (3, 6]) as the first interval and the corresponding cluster as the first cluster. Similarly, the intervals (1.5, 3] and [1, 1.5] are referred to as the second and third intervals and the corresponding clusters as the second and third clusters, respectively.

With this clustering approach, the ratio between the maximal and the minimal energy consumption rates of nodes in the same cluster is upper bounded by α. Clearly, α plays a critical role in determining the charging performance. We will elaborate the optimal setting of α in Section IV-E, and our evaluation results in Section VIII indicate that an α of 2 leads to the best performance in most cases.

B. Nested Tour Construction

The next step is to construct TSP tours according to the m clusters in a nested manner. We construct m TSP tours based on the first i clusters $(i = 1, 2, \ldots, m)$ and denote these tours as $\{T^1_{\text{tsp}}, T^2_{\text{tsp}}, \ldots, T^m_{\text{tsp}}\}$. Because the tours are constructed in a nested manner, their length satisfies the following relationship:

$$\left|T^1_{\text{tsp}}\right| \leq \left|T^2_{\text{tsp}}\right| \leq \left|T^3_{\text{tsp}}\right| \leq \cdots \leq \left|T^m_{\text{tsp}}\right|. \tag{3}$$

In the example shown in Fig. 4, three nested TSP tours are constructed based on these three node clusters. The shortest tour T^1_{tsp} is shown in Fig. 4(1), the second shortest tour T^2_{tsp} is shown in Fig. 4(3), and the longest tour T^3_{tsp} is shown in Fig. 4(7).

When nodes near the sink have higher energy consumption rates, which is a typical case for multihop sensor networks, the nodes in the same cluster are also relatively close in the spatial dimension. This spatial-correlated energy consumption pattern facilitates the energy synchronization of nodes in the same cluster and, thus, improves the performance of our design. However, even in networks without this energy consumption pattern, our design still outperforms existing solutions significantly, which we will further investigate in Section VIII.

[4]Note its difference with the traditional operator $\lceil x \rceil$ when x is an integer.

$$
\begin{aligned}
0 &= 0\times 2^0 + 0\times 2^1 + 0\times 2^2 \quad \rightarrow \quad \mathcal{C}_0 = <0,0,0>,\\
1 &= 1\times 2^0 + 0\times 2^1 + 0\times 2^2 \quad \rightarrow \quad \mathcal{C}_1 = <1,0,0>,\\
2 &= 0\times 2^0 + 1\times 2^1 + 0\times 2^2 \quad \rightarrow \quad \mathcal{C}_2 = <0,1,0>,\\
3 &= 1\times 2^0 + 1\times 2^1 + 0\times 2^2 \quad \rightarrow \quad \mathcal{C}_3 = <1,1,0>,\\
4 &= 0\times 2^0 + 0\times 2^1 + 1\times 2^2 \quad \rightarrow \quad \mathcal{C}_4 = <0,0,1>.
\end{aligned}
$$

Fig. 5. Tour selection based on the sum expression in (4).

C. Tour Selection for Each Round

With the nested TSP tours, the mobile charger periodically carries out the charging tasks by selecting one of these nested tours in each round and charges the nodes involved in the tour if necessary. Thus, the next question we need to decide on is: Which tour the mobile charger should select for a given round of the on-demand charging process? We emphasize that the tour selection in our design is just to provide guidance in the scheduling of the charging tasks during that round, and it is not necessary for the charger to visit all nodes along the tour, which we will explain in detail in Section V.

1) Key Observation: Again, before introducing our design on the tour selection algorithm, we first use the example shown in Fig. 4 to present our basic idea. With the *power-*α clustering algorithm and the tour construction method previously introduced, we obtain three node clusters (i.e., square, triangle, and circle) and three nested TSP tours [i.e., T^1_{tsp}, T^2_{tsp}, and T^3_{tsp} as in Fig. 4(1), (3), and (7)]. For the mobile charger, it is desirable to select the shortest TSP tour containing all the energy depleted nodes in each charging round. In the first round of the charging process, only the square nodes deplete their energy supply, and thus, the charger would prefer to select the shortest tour containing the square nodes, i.e., T^1_{tsp}, as the tour to guide the charging process [see Fig. 4(1)]. Similarly, in the second round, the charger would prefer to select the shortest tour containing the square and triangle nodes, i.e., T^2_{tsp}, to follow [see Fig. 4(3)]. T^1_{tsp} is selected again in the third round since now, only the square nodes are out of energy supply [see Fig. 4(5)]. Then, in the fourth round, all nodes deplete their energy supply, and the TSP tour containing all of them is selected [see Fig. 4(7)]. From this example, we can see that the tour selection algorithm is expected to identify the shortest TSP tour containing all the energy-hungry nodes in each charging round, and the following observation inspires us with the solution.

For any given α and m, every $j \in \{0, 1, \ldots, \alpha^{m-1}\}$ can be represented in the form of

$$j = \sum_{i=0}^{m-1} c_i^j \cdot \alpha^i \tag{4}$$

where $c_i^j \in \{0, 1, \ldots, \alpha - 1\}$. To clearly demonstrate the relationship between the selected tour in the jth round and j's sum expression in (4), let us define an ordered set $\mathcal{C}_j = \langle c_0^j, c_1^j, \ldots, c_{m-1}^j \rangle$. For ease of description, further define $\mathcal{C}_0 = \langle 0, 0, \ldots, 0 \rangle$ and $|\mathcal{C}_0| = m - 1$. Then, with $\alpha = 2$ and $m = 3$, the sum expressions and the corresponding $\mathcal{C}_j$ for the first four rounds of the mobile charging process are shown in Fig. 5.

We can see that in the first round, the only element in $\mathcal{C}_1$ that is larger than the corresponding element in $\mathcal{C}_0$ is the first element, and from the example in Fig. 4, we know that the first tour (i.e., T^1_{tsp}) is desirable to be selected in the first round. For the second round, the second element in $\mathcal{C}_2$ is larger than the second element in $\mathcal{C}_1$, and on the other hand, the second tour T^2_{tsp} is desirable to be selected in the second round. This agreement holds for the third and fourth rounds as well. For the third round, the first element in $\mathcal{C}_3$ is larger than that in $\mathcal{C}_2$, and the desirable tour is T^1_{tsp}. For the fourth round, the third element in $\mathcal{C}_4$ is larger than that in $\mathcal{C}_3$, and the desirable tour is T^3_{tsp}.

This relationship between the tour selected in the jth round and j's sum expression inspires us with the design of the tour selection algorithm.

2) Tour Selection Algorithm Design: For a given round index $j \in \{1, 2, \ldots, \alpha^{m-1}\}$, we first identify the corresponding $\mathcal{C}_j$. Then, we compare it with $\mathcal{C}_{j-1}$ and find the k ($k = 0, 1, \ldots, m-1$) such that $c_k^j > c_k^{j-1}$. The following theorem shows that one and only one such k can be found for every round index j.

Theorem 1: For a given α, m, and round index j, there exists one and only one k such that: $c_k^j > c_k^{j-1}$.

Proof: For any j and $j+1$ $j \in [1, 2, \ldots, \alpha^{m-1}]$, they can be represented by

$$
\begin{aligned}
j &= c_0^j\alpha^0 + c_1^j\alpha^1 + \cdots + c_{m-1}^j\alpha^{m-1}\\
j+1 &= c_0^{j+1}\alpha^0 + c_1^{j+1}\alpha^1 + \cdots + c_{m-1}^{j+1}\alpha^{m-1}
\end{aligned}
$$

and thus, we have

$$\sum_{i=0}^{m-1} \left(c_i^{j+1} - c_i^j\right)\alpha^i = 1$$

which means that at least one of $(c_i^{j+1} - c_i^j)$ is larger than 0. This proves the existence of k.

To prove k's unique existence, we observe the fact that

$$j + 1 = \left(c_0^j + 1\right)\alpha^0 + c_1^j\alpha^1 + \cdots + c_{m-1}^j\alpha^{m-1}.$$

Then, if $c_0^j < \alpha - 1$, we have $c_0^{j+1} = c_0^j + 1$, and $c_i^{j+1} = c_i^j$ for all $i \in [1, 2, \ldots, m-1]$. Otherwise, we have $c_0^{j+1} = 0$, $c_1^{j+1} = c_1^j + 1$, and $c_i^{j+1} = c_i^j$ for all $i \in [2, \ldots, m-1]$. This way, we can see that once a k such that $c_k^{j+1} > c_k^j$ has been found, then $\forall k' \in [0, 1, \ldots, k-1]$, $c_{k'}^{j+1} = 0$, and $\forall k'' \in [k+1, k+2, \ldots, m-1]$, $c_{k''}^{j+1} = c_{k''}^j$. Thus, the unique existence of k is proved. ■

As a result, the charger takes the $(k+1)$th tour in the jth round. The sequence of the adopted tours repeats every α^{m-1} rounds.

We can see that with the proposed tour construction and selection algorithms, for each round of the charging process, the charger always selects the shortest TSP tour that contains all the sensor nodes with low remaining energy levels. As a result, the charger travel distance during the charging process is reduced.

D. When to Start a New Round

During the mobile charging process, a clear trigger to start a new round is when all the requesting nodes involved in the current tour have been charged, and the node with the highest energy consumption rate has requested charging again.

Another event that triggers the start of a new round is the reception of charging requests from nodes not involved in the current round. In this case, to reduce the energy depleted duration of these nodes, the mobile charger needs to start a new round (i.e., increase j by 1) and reselect the adopted tour. This process continues until all the requesting nodes are involved in the adopted tour.

From the first trigger, we can see the longest time that a round can last is dominated by the time between two consecutive charging requests of the node with the highest energy consumption rate, which is upper bounded by $E/r_{\max}$, where E is the nodes' capacity when fully charged.

E. Determining the Optimal Power Factor

We have introduced how to construct the nested TSP tours and which tour to select for each charging round with a given power factor α. Next, we explain how to identify the optimal setting of α. The power factor α directly affects the constructed TSP tours, and its optimal setting is jointly determined by the nodes' energy consumption rates and their locations. This means that identifying the optimal α before network deployment is challenging. However, once at least one charging request has been received from each node, both the estimated energy consumption rates and node locations can be made available to the charger, e.g., by piggybacking the information in the charging requests, based on which the optimal α can be identified.

For ease of description, we extend our previous notation on T^i_{tsp} by denoting the ith TSP tour obtained with a specific α as $T^i_{\text{tsp}(\alpha)}$. Denote m_α as the number of clusters obtained with power factor α. With the proposed tour selection algorithm, the sequence of adopted tours will repeat every $\alpha^{m_\alpha-1}$ rounds. The worst-case charger travel distance during these rounds Y_α is

$$Y_\alpha = \left|T^{m_\alpha}_{\text{tsp}(\alpha)}\right| + \sum_{i=1}^{m_\alpha-1} \alpha^{m_\alpha-i-1} \left|T^{i}_{\text{tsp}(\alpha)}\right|$$

and thus, an upper bound Z_α of the asymptotic average travel distance for each round is

$$Z_\alpha = Y_\alpha/(\alpha^{m_\alpha-1}).$$

Then, the mobile charger can adopt the α with the minimum Z_α to carry out the charging tasks, i.e.,

$$\hat{\alpha} = \{\alpha : \min\{Z_\alpha\}\}.$$

Note that when $\alpha > r_{\max}/r_{\min}$, only one cluster containing all the nodes will be formed, and *ESync* regresses to the simple case where only the TSP tour containing all nodes is involved in the charging process. Thus, the charger only needs to check the potential value of α in $[2, r_{\max}/r_{\min}]$ to determine its optimal setting.

F. Time Complexity

We need a time of $\mathcal{O}(m_\alpha C_{\text{tsp}})$ to accomplish the node clustering and tour construction with a specific α, where C_{tsp} is the time complexity to obtain the near-optimal TSP tour. As previously mentioned, the charger needs to check, at most, $((r_{\max}/r_{\min})-1)$ possible values of α to determine the optimal setting. As a summary, the computation complexity in constructing the nested TSP tours is $\mathcal{O}(C_{\text{tsp}}(r_{\max}/r_{\min})\log(r_{\max}/r_{\min}))$. The charger needs a time of $\mathcal{O}(\log_\alpha(r_{\max}/r_{\min}))$ to select the tour in each round.

V. Energy Synchronization Among Nodes

With the nested TSP tours and the tour selection method, only energy-hungry nodes are involved in each charging round. Here, we further improve the charging process by synchronizing the energy supply of nodes to proactively adjust their charging request sequence. As a result, the charging request sequence of nodes is synchronized with their sequence on the TSP tours. Specifically, if the charging requests from two neighboring nodes are sent out according to their sequence on the selected TSP tour, we say that these two nodes are *energy synchronized* in the charging process. This energy synchronization among nodes is achieved by carefully controlling the amount of energy charged to individual nodes.

In general, the mobile charger needs to address two questions to carry out the charging process in each round: Which node should be charged next, and how much energy should be charged to the node.

A. Which Node to Charge Next

In our design, the node to be charged next is determined according to the selected TSP tour in each round. Specifically, after completing the charging of the current node, the mobile charger selects the requesting node that is closest to its current location along the TSP tour as the next node to charge.

Although, our method demonstrates a greedy feature, which may cause the unfairness issue among sensor nodes. Because we only apply the greedy feature based on the TSP tour, the potential unfairness issue is significantly alleviated.

B. How Much to Charge

To achieve the energy synchronization among nodes, the charger does not always fully charge individual nodes, and then, we explain how to determine the amount of energy charged to the selected node. In our design, we determine the amount of energy charged to individual nodes with the objective of synchronizing their energy supply. Thus, given the selected charging node, we first need to identify the node to which to synchronize its energy, i.e., its *synchronization target*.

Assume that the mobile charger is currently working in the jth round following tour $T^{f(j)}_{\text{tsp}}$, where $f(j)$ is the tour

index returned by the tour selection algorithm. To find the synchronization target of a given node s in this round, which belongs to the ith cluster, we first identify the round j' in which s is involved the next time by

$$j' = j + \alpha^{i-1} \quad (i = 1, 2, \ldots, m). \tag{5}$$

The adopted tour in the j'th round, i.e., $T_{\text{tsp}}^{f(j')}$, can be calculated by the tour selection algorithm. Then, we find the previous node of s along $T_{\text{tsp}}^{f(j')}$ as the synchronization target of s in the jth round, which is denoted as u for ease of description. This is because the desired effect that is to be achieved is when s requests energy replenishment the next time the mobile charger has just accomplished the charging of u in the j'th round, which means that the energy of s is synchronized with u in the j'th round.

Two pieces of information are needed to calculate the amount of charged energy to achieve the energy synchronization between s and u: the energy consumption rates of s and u and the time duration until u is charged in the j'th round.

The nodes' energy consumption rates can be estimated based on the history of charging requests. As an example, the energy consumption rate of a specific node can be estimated based on its operation time with a single full charging [45]. We emphasize again that the perfect estimation is extremely challenging, and our design does not require the perfect estimation of the nodes' energy consumption rates, as will be shown in Sections VII and VIII.

Next, we explore the time duration until u is charged in the j'th round. The number of rounds that u is involved between the jth and the j'th round can be calculated in a similar manner as (5) and denote it as q. The total amount of energy charged to u in these q rounds is, at most, qE, and thus, the time from now until u requests charging in the j'th round is, at most, $(qE + e_r(u))/r(u)$, where $e_r(u)$ is the current remaining energy of u, and $r(u)$ is its energy consumption rate.

As a result, the amount of energy charged to s is calculated according to

$$e(s) = r(s)\left(\frac{qE + e_r(u)}{r(u)} + t_c\right) - e_r(s) \tag{6}$$

where t_c is the worst-case charging time to fully replenish the nodes' energy supply (i.e., the longest possible time to charge u in the j'th round), and thus, $((qE + e_r(u)/r(u)) + t_c)$ is the time before the charger arrives to charge s the next time. Note that $e(s) \in [0, E - e_r(s)]$.

Determining the amount of charged energy according to (6) indicates that the charger would not always fully charge individual nodes. However, this occasional partial charging of nodes facilities the energy synchronization among nodes, and thus, the overall charging performance outperforms that when the charger always fully charges nodes. Specifically, from our evaluation results in Section VIII, we observe a 30% and 40% reduction in the charger travel distance and the charging delay of sensor nodes, respectively.

During the charging process in each round, the charger needs a time of $\mathcal{O}(n)$ to determine the next node to charge, and another time of $\mathcal{O}(\log_\alpha(r_{\max}/r_{\min}))$ is needed to determine the amount of charged energy.

C. Periodic Charging Process

Next we will show that the aforementioned mobile charging protocol leads to a periodic sequence of the TSP tour selected under the ideal case.

Theorem 2: Consider the *ESync protocol*, where the amount of energy charged is computed by (6). Assuming that the energy consumption rate $r(u)$ is perfectly estimated and ignoring the worst-case charging time t_c, the selected TSP tours converge to be periodic.

Proof: We model the TSP selection and energy charging process as a Markov decision process (MDP). The state of the MDP is the remaining energy $e_r(u)$, and the action is the amount of energy charged $e(s)$. The transition probabilities are either 1 or 0 since $e(s)$ is computed by (6), at each round $e_r(u)$ is a multiple of $r(u)$, i.e., there exists an integer β such that $e_r(u) = \beta r(u)$. On the other hand, $e_r(u) \leq E$, where E is the node capacity when fully charged. Therefore, the state space of the MDP is finite. Ignoring the worst-case charging time t_c, the action space of the MDP is also finite by (6). There must exist some states that are recurrently reached, which completes the proof. ■

Through testbed experiments and numerous simulation results in Sections VII and VIII, this periodic charging process is demonstrated, as shown in Figs. 10 and 15.

VI. Further Discussion

A. Sufficient Condition to Achieve Energy Synchronization

The core idea of *ESync* is to synchronize the nodes' energy according to their sequence on TSP tours. Clearly, if the energy synchronization is achievable, it means that in the worst case, there is enough time for the charger to complete the charging tasks of all nodes included in each round. In other words, the time for the charger to perform one round of the charging tasks must be smaller than the shortest node lifetime in the network.

As mentioned in Section IV-D, the longest time that a round can last is $E/r_{\max}$. Furthermore, it is clear that the round requiring the longest time is that during which T_{tsp}^m is adopted. It has been shown that a lower bound of the TSP tour length in an $L \times L$ square field with n randomly deployed nodes is [49]

$$\left|T_{\text{tsp}}^m\right| \geq L\sqrt{n/2}. \tag{7}$$

Thus, the longest travel time during each round is lower bounded by $(L/v)\sqrt{n/2}$. Incorporating the worst-case charging time to replenish all the n nodes, a *sufficient condition* for the energy synchronization to be achievable is

$$E/r_{\max} \geq L\sqrt{n/2}/v + nt_c. \tag{8}$$

Because it is not necessary for the charger to visit and charge all nodes during each round, (8) is not a *necessary condition*. When the sensing field cannot be approximated by a square, (8) can be extended by substituting (7) accordingly.

B. Advantage of ESync Over Classic Solutions

The advantage of *ESync* over the TSP-based protocols is straightforward. The charger does not visit nodes with sufficient energy supply with *ESync*, and thus, its travel distance is reduced, which, in turn, shortens the charging latency of nodes.

The comparison between *ESync* and Nearest-Job-Next is more complicated due to the randomness in the network; thus, we consider an ideal case where the energy synchronization is perfectly achieved. In this case, the sequence that sensor nodes send out their energy replenishment requests is consistent with their sequences on the TSP tour, and thus, the mobile charger will travel along the TSP tour to perform the charging tasks during each round. As a result, the charger travel distance during each round is exactly the length of the TSP tour. On the other hand, the asymptotic lower bound of the charger travel distance under Nearest-Job-Next is the length of the corresponding greedy path, which is clearly longer than the optimal TSP tour. Again, the shorter travel distance under *ESync* indicates a shorter charging latency of sensor nodes.

C. Charger Energy Replenishment

Although, usually, the mobile charger has much larger energy capacity than sensor nodes, the energy replenishment of the charger itself also needs to be considered in practical implementations, particularly when the deployment field or the number of deployed nodes is large. *ESync* can seamlessly incorporate the energy replenishment of the charger into the charging process. Assume there is an energy tank from which the charger energy can be replenished. Whenever the energy level of the charger is low, we treat it as a *virtual charging request* initiated by the energy tank. The energy tank can be included into the *power-*α clustering algorithm based on the charger's operation time with a single charge, just as a usual sensor node. As a result, the charger's energy replenishment can be handled in the same way as those for sensor nodes.

The performance of the mobile charging process cannot be guaranteed in certain situations such as when the time to charge the battery is long or when the node density is quite high. Employing more chargers to collaboratively charge the nodes is necessary in such cases. Wang *et al.* in [50] proposed an efficient approach to partition the network with which a carefully selected subset of nodes is assigned to individual chargers. This partitioning algorithm can be adopted to extend *ESync* to the case of multiple chargers—after partitioning the network, for each charger, *ESync* is applied to the subset of the nodes assigned to that charger, based on which the mobile charging process is performed.

VII. Experiment Evaluation

We evaluate the performance of *ESync* through both experiments and simulations. The experimental results are presented in this section, and the insights obtained through large-scale simulations will be introduced in the following section.

In our experiment, we randomly deploy nine sensor nodes in an open field of 3×3 m^2, and a LEGO Mindstorms NXT robot

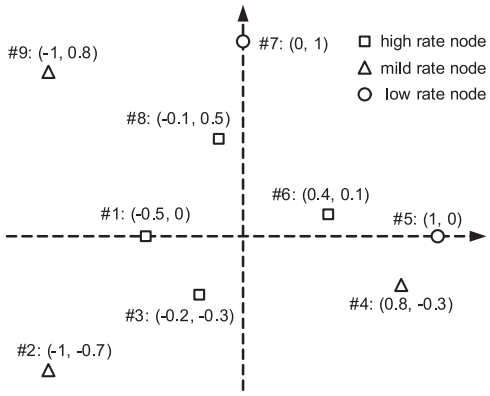

Fig. 6. Node locations.

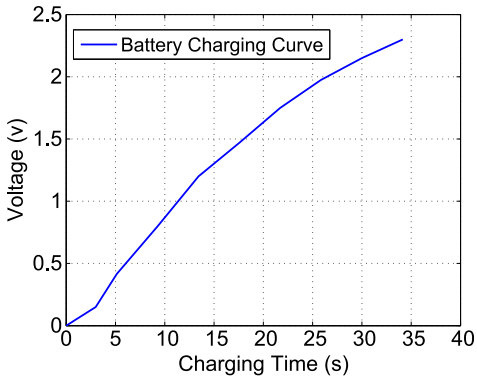

Fig. 7. Typical battery charging curve [51].

with an average travel speed of 0.1 m/s is adopted as the mobile charger. The locations of these nodes are shown in Fig. 6.

Fig. 7 shows the relationship between battery voltage and charging time [51]. The battery can be charged with a steady curve in the charging stage, during which the battery voltage and the charging time clearly demonstrate a close-to-linear relationship (as shown in Fig. 7). Similar charging curves are reported in the data sheets of off-the-shelf battery products [52]. Based on this observation, we implement a simple linear charging model to emulate the charging of nodes. Specifically, the time to accomplish the charging of a specific node s is calculated by

$$\text{charging time} = \frac{e(s)}{E} t_c$$

where $e(s)$ is the amount of energy charged to s, E is the full energy capacity of nodes, and t_c is the time to fully charge an energy depleted node. This simplified charging model is sufficient for our evaluation purpose, particularly when not all the nodes are fully charged in our energy synchronized charging design (which avoids the nonlinear portion of the charging curve). Specifically, we emulate a scenario where $E = 100$ units and the charging rate of the charger is 30 units per second, indicating the worst-case charging time $t_c = 400/120 \approx 3.3$ s. The average energy consumption rates of nodes are shown in Table I. The rationale behind these settings is that because of our limited testbed size (i.e., 3×3 m^2, as previously stated),

TABLE I
AVERAGE ENERGY CONSUMPTION RATES

Node	#1	#2	#3	#4	#5	#6	#7	#8	#9
r_i	4	2	4	2	1	4	1	4	2

TABLE II
SCALE DOWN A REALISTIC NETWORK TO THE EXPERIMENT SETTINGS

	Envisioned Network	Experiment
Network Area	$1,000 \times 1,000\ m^2$	$3 \times 3\ m^2$
Nodes Lifetime	10–40 hours	100–400 s
Fully Charge Time	20 min	3.33 s

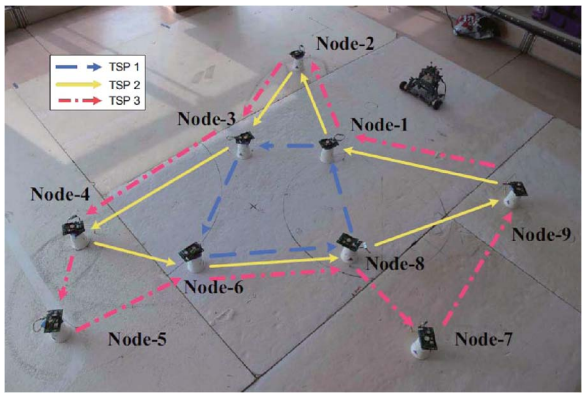

Fig. 8. Overview of the experiment settings.

we need to scale down a realistic network in both the spatial and temporal dimensions. Specifically, we envision a network area of 1,000 × 1,000 m^2, where the average node lifetime is about 10–40 h upon fully charged. The charger needs a charging time of about 20 min to fully charge an energy-depleted node, as with the commercial fast charger for AA batteries commonly adopted in sensor nodes. Then, we map the considered network area to our experiment field and scale down other settings accordingly, as summarized in Table II. These nine sensor nodes are organized into three clusters based on their energy consumption rates (i.e., {1, 3, 6, 8}, {2, 4, 9}, and {5, 7}), and three nested TSP tours are constructed accordingly, as highlighted in Fig. 8. Sensor nodes send out charging requests to the charger when their energy supply is depleted, and the charger carries out these charging tasks according to *ESync*.

We evaluate the performance of *ESync* and compare it with two classic baselines: TSP [17] and Nearest-Job-Next [31], upon which most existing designs are based [17]. For TSP, the charger travels and charges nodes following the TSP tour, and its travel is independent of whether the charging request from the node has been received. With TSP, the charger periodically visits sensor nodes according to preoptimized TSP tours. Upon its arrival at a particular node, the charger will replenish the node energy supply if the node has sent out a charging request, or it will skip to visit the next node otherwise. For Nearest-Job-Next, the charger always selects the geographically nearest requesting node as the next node to charge. Both these two baselines adopt the full charging of nodes throughout the charging process.

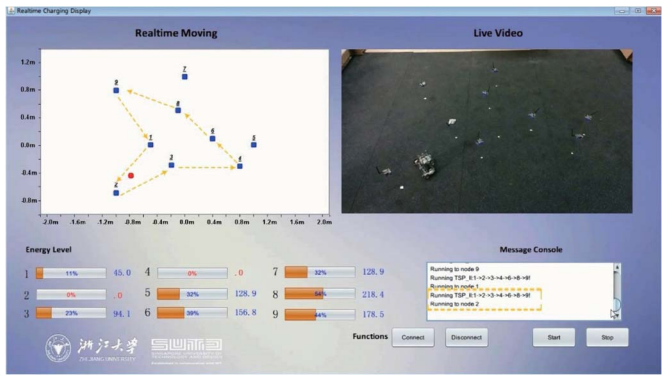

Fig. 9. Demonstration of the mobile charging process.

To capture the fact that the nodes' energy consumption rates are usually dynamic in practice, we introduce an estimation error parameter ϵ ($\epsilon \in [0, 1]$) to generate the actual energy consumption of nodes in each second. Specifically, the energy consumption of node-i in each second is randomly generated in

$$[(1-\epsilon)r_i, (1+\epsilon)r_i] \tag{9}$$

where r_i is the average energy consumption rate of node-i, as shown in Table I.[5]

A mobile charging process of 15 min is performed in each experiment, and the request charging delay and charger travel distance during these charging processes are recorded for evaluation. To better visualize the mobile charging process, Fig. 9 shows a testbed snapshot of the online demo display during the mobile charging process. A video demonstrating the experimented mobile charging process can be found at http://www.youtube.com/watch?v=2em2cJZDdMU.

We understand that if possible, the average *delay per request* could offer additional information than the total charging delay. However, the reason for adopting the latter as the evaluation metric is that with *ESync*, the charged nodes consist of two categories: the nodes that have requested charging and the nodes that have not sent out charging requests but are charged to synchronize their energy supply. Note that with both NJN and TSP, the charger charges only the nodes that have sent out charging requests. This way, the metric of average *delay per request* may lead to biased observations and, thus, is not adopted in our evaluation (see Figs. 10 and 11).

The charger travel distance and request charging delay resultant with ϵ varying from 0% to 30% are shown in Figs. 12 and 13, respectively. We can see that the charger travel distance resultant by *ESync* is about 30% and 20% shorter than those obtained by TSP and Nearest-Job-Next, and the request charging delay is reduced by about 50%. Furthermore, we can see that although the performance of *ESync* degrades with a larger estimation error on the nodes' energy consumption rates, it still noticeably outperforms both TSP and NJN even with an ϵ as large as 30%, indicating good tolerance of *ESync* on the energy consumption variance of sensor nodes.

[5]However, we assume a perfect estimation on the nodes' energy consumption rates for TSP and Nearest-Job-Next.

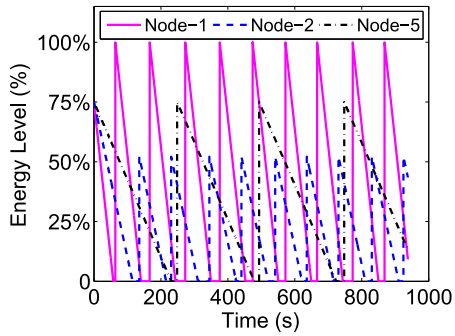

Fig. 10. Evolution traces of the nodes' remaining energy levels during the experiment.

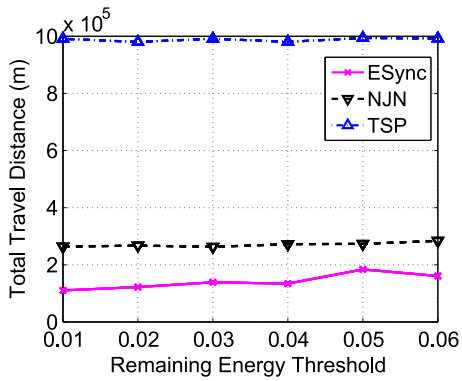

Fig. 11. Impact of the remaining energy threshold to trigger the charging requests.

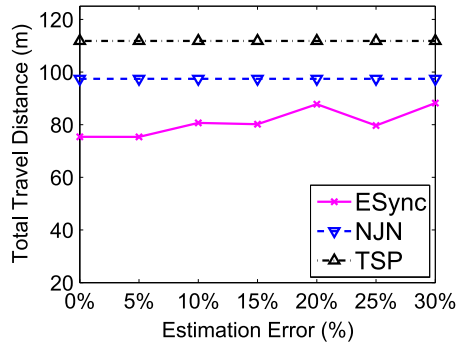

Fig. 12. Charger travel distance with estimation error on the nodes' energy consumption rates.

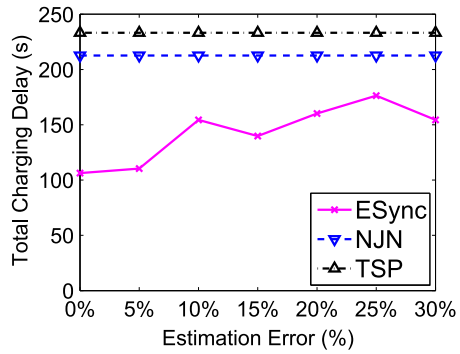

Fig. 13. Charging delay with estimation error on the nodes' energy consumption rates.

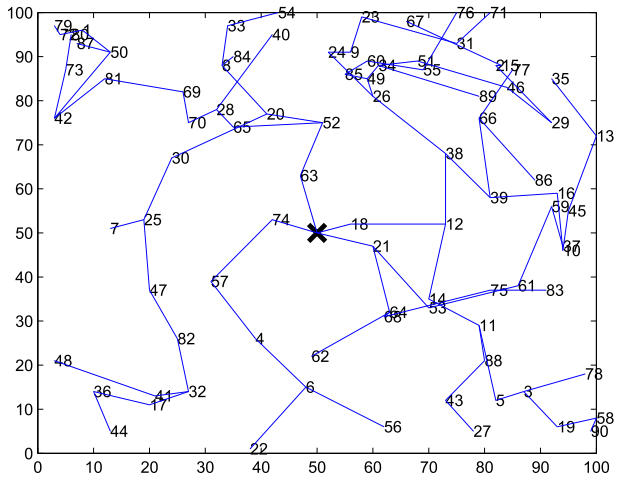

Fig. 14. Sample routing structure in our simulations.

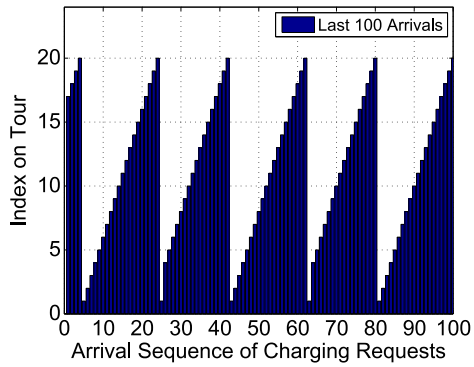

Fig. 15. Visualizing the effect of energy synchronization.

To clearly illustrate the evolution of the nodes' remaining energy during a mobile charging process of 15 min, we show the energy level of node-1, node-2, and node-5 in Fig. 10, i.e., one for each of the three node clusters. We can see that node-1 is always charged to its full capacity because it has the highest energy consumption rates (and thus the shortest lifetime) in the network, whereas node-2 and node-5 are only partially charged. Furthermore, the frequencies for the three nodes to be charged decrease with the order of node-1, node-2, and node-5. This is because node-1 is involved in all three nested TSP tours, whereas node-5 is only involved in the third tour, as shown in Fig. 8.

VIII. Simulation Evaluation

Here, we evaluate the performance of *ESync* through extensive simulations.

A. Simulation Setup

We simulate an environment monitoring sensor network with 20–200 randomly deployed nodes. The sensing field size varies from 60 m × 60 m to 160 m × 160 m, and a sink is located at the field center. The nodes' communication range is 20 m to form a multihop network topology. The nodes' energy capacity is

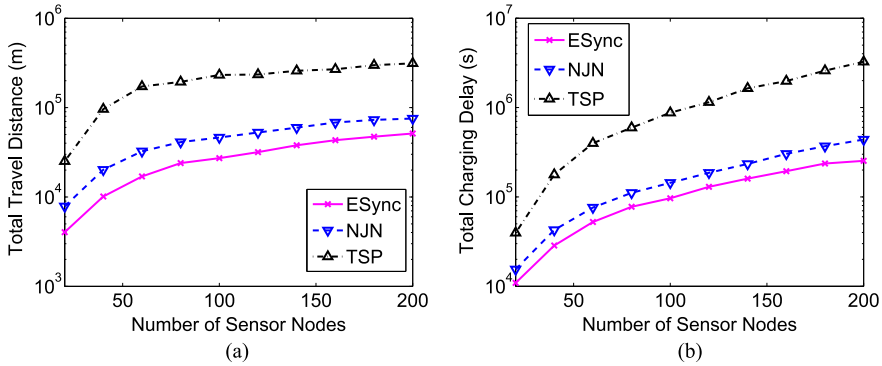

Fig. 16. Impact of n on the charging process. (a) Total travel distance. (b) Total charging delay.

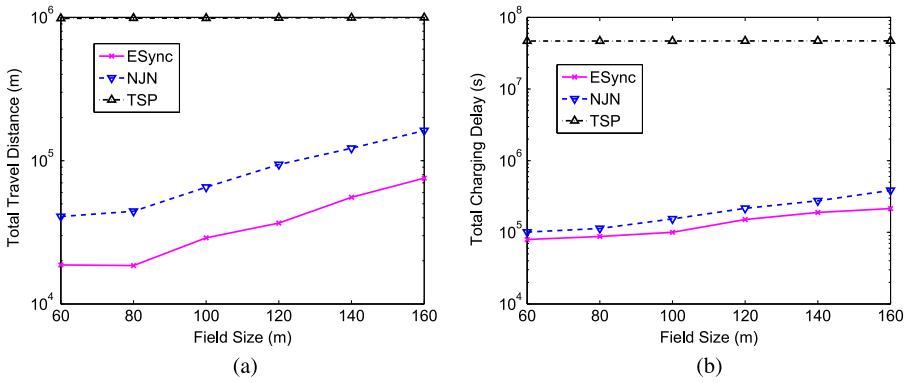

Fig. 17. Impact of L on the charging process. (a) Total travel distance. (b) Total charging delay.

1000 mAH. The energy consumption rate for the sensing tasks is 0.75 mA $\times$ 2 V $=$ 1.5 mW, which is typical for a light sensor [53]. The communication energy costs of sensor nodes are set based on the data sheet of MICA2 node: With transmitting and receiving current draw of 25 and 8 mA, respectively, the corresponding energy consumption rates are 25 mA $\times$ 2 V $=$ 50 mW and 8 mA $\times$ 2 V $=$ 16 mW with a typical voltage of 2 V. After node deployment, a routing structure is constructed based on the TinyOS standard CTP [54]. Then, the environment information, after being captured by individual nodes, is transmitted to the sink through multihop communications. Sensor nodes send out charging requests to the charger when their remaining energy approaches zero. In our event-driven simulator, the sensory data are simulated as events occurred at random time and random locations—whenever an event happens in the sensing range of sensor nodes, these nodes would capture the event in different details and transmit the data to the sink via the constructed routing structure. This way, we do not take the data rates of sensors as control parameters in our simulation, but generate them according to the event occurrence rates. It is true that under such a scenario, the nodes near the sink would have higher energy consumption rates, which can be inferred from Fig. 14, showing the routing structure of a particular node deployment in our simulations. The charger travel speed is 1 m/s, unless otherwise specified [42]. We simulate a network operation period of 500 000 s and record the total distance that the mobile charger traveled and the total charging delay of sensor nodes. We adopt *Concorde* [44], which is an open-source TSP solver with verified efficiency, to obtain the near-optimal TSP tours in our simulation. The mobile charging process is simulated with MATLAB.

B. Visualizing the Effect of Energy Synchronization

Before evaluating the performance of *ESync*, we first run *ESync* on the same setting as in Fig. 2 to visualize the effect of energy synchronization when only a single TSP tour is constructed. With a simulated time of 500 000 s, during which a total number of 948 charging requests are served, the last 100 requests in the simulation are shown in Fig. 15.

Compared with Fig. 2, we can see that although the realization of energy synchronization is not yet perfect due to the dynamics in the charging process, the request sequence greatly matches the TSP tour, and thus, our design is validated. Furthermore, we observe that the effect of energy synchronization begins to show as early as from the 200th to 300th requests, indicating a short time to achieve the energy synchronization.

C. Performance Evaluation

1) Impact of Network Scale: To investigate the scalability of *ESync*, we evaluate its performance with different network scales with respect to the number of deployed sensor nodes. The resultant charger travel distance and charging delay of sensor nodes are shown in Fig. 16(a) and (b), respectively, where the number of nodes varies from 20 to 200. Note that due to the

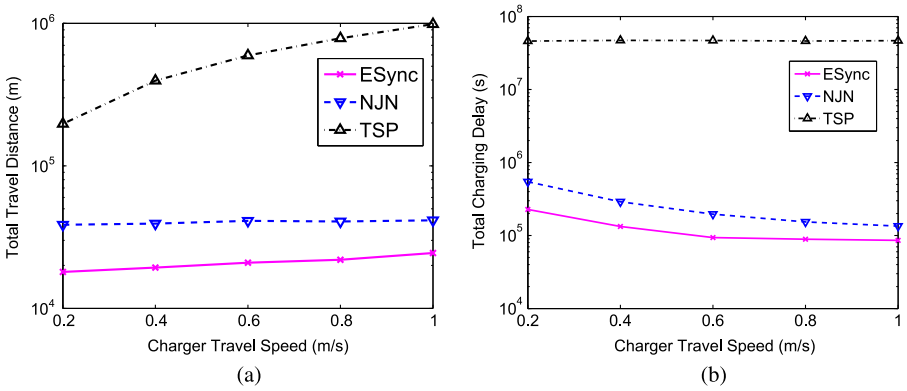

Fig. 18. Impact of v on the charging process. (a) Total travel distance. (b) Total charging delay.

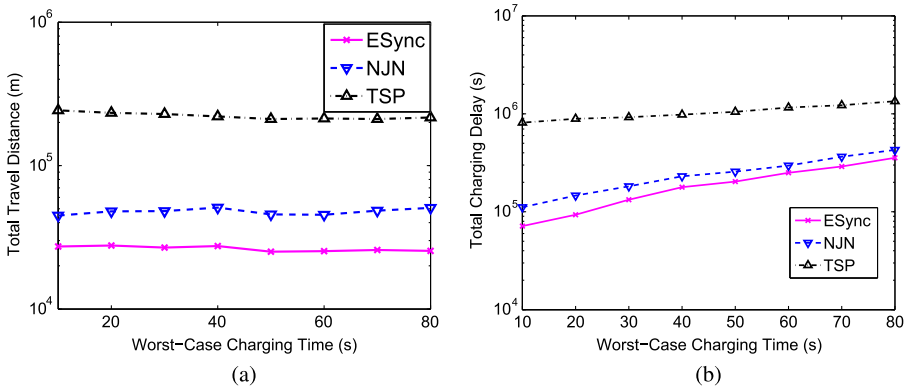

Fig. 19. Impact of t_c on the charging process. (a) Total travel distance. (b) Total charging delay.

large gap among the results returned by the three charging protocols, the y-axis in the figures is in *log-scale*. We can see that *ESync* achieves the best performance for all the network scales investigated. For example, the charger travel distance (charging delay of nodes) resultant with *ESync* is about 58.78% (67.11%) of that returned by Nearest-Job-Next when 100 nodes are deployed. When compared with TSP, the two ratios are further reduced to 11.73% and 11.03%, respectively. Fixing the number of nodes as 100, we evaluate the performance of *ESync* with varying deployment field sizes, as shown in Fig. 17(a) and (b). Again, *ESync* demonstrates an obvious advantage over the two baselines for all the explored settings, and an average reduction of around 57% in the charger travel distance and 30% in the charging latency of nodes can be observed when compared with Nearest-Job-Next.

The charging performance degrades as the network scale increases. Thus, multiple chargers may be needed in large-scale networks. We will further investigate the collaborative mobile charging process in our future work.

2) Impact of Charger Travel Speed: An important factor that determines the charger's ability in performing charging tasks is its travel speed v. We explore the performance of *ESync* with varying charger speeds from 0.2 to 1 m/s. The resultant charger travel distance and energy depletion duration of nodes are shown in Fig. 18(a) and (b), respectively. The advantage of *ESync* can be clearly observed. The charger travel distance increases with a larger v, because the charger can accomplish more charging tasks in this case. Furthermore, because the charger can accomplish charging tasks faster, the energy depletion duration of nodes is reduced as well.

3) Impact of Charging Time: Another factor that affects the charger's charging ability is the worst-case charging time t_c. With t_c varying from 10 to 80 s, the evaluation results on the total charger travel distance and the total energy depletion duration of nodes are shown in Fig. 19(a) and (b), respectively. We can see that the advantage of *ESync* over the two baselines is obvious. The charger travel distance and the energy depletion duration of nodes are averagely reduced to 57.74% and 63.76% of those with Nearest-Job-Next, respectively. When compared with TSP, the two ratios are further reduced to 11.88% and 10.89%, respectively. The charger travel distance decreases as t_c increases, because the charger needs to spend more time to charge nodes. Note that this decrease in charger travel distance is not because the charger can more *effectively* carry out the charging tasks when t_c becomes larger. In contrast, it is due to the decrease in the charger's ability to perform the charging tasks.

4) Impact of Power Factor: The power factor α directly affects the performance of *ESync*. From our simulation results, we observe that a power factor of 2 is adopted for most of the time. To further investigate the impact of α, we fix the network scale at 100 nodes in a 100 m $\times$ 100 m field and explore *ESync* with α varying from 2 to 6. The results are shown in Fig. 20(a) and (b). A clear increasing trend of the travel distance and the

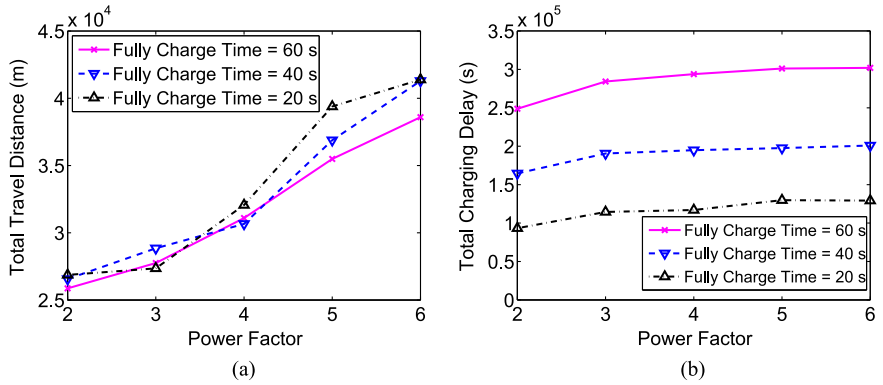

Fig. 20. Impact of α on the charging process. (a) Total travel distance. (b) Total charging delay.

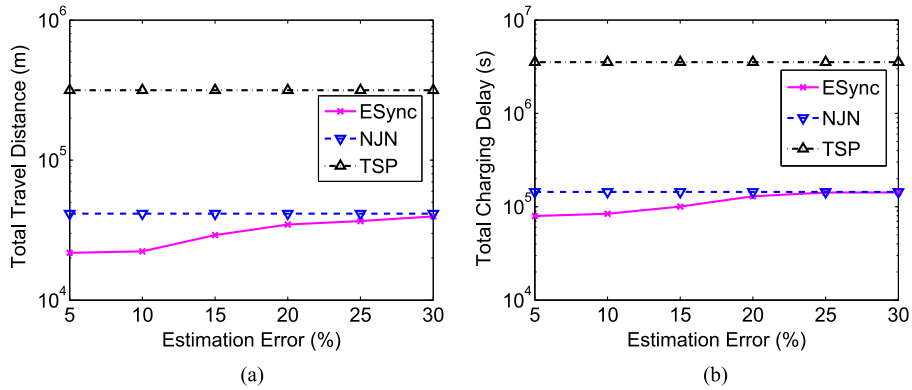

Fig. 21. Impact of ϵ on the charging process. (a) Total travel distance. (b) Total charging delay.

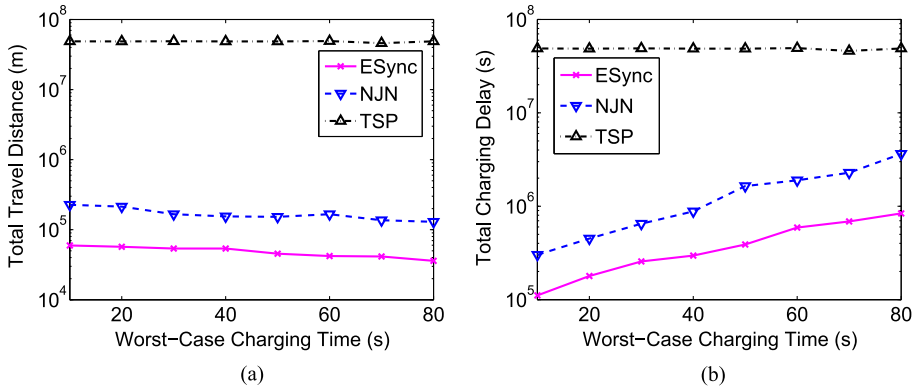

Fig. 22. With spatially random consumption. (a) Total travel distance. (b) Total charging delay.

charging delay can be observed as α becomes larger, which agrees with our observation and, thus, validates our method in determining the optimal α.

5) Impact of Estimation Errors: In real network applications, variance exists in the nodes' energy consumption, and thus, the estimated energy consumption rates and remaining energy would not be perfectly accurate. With a t_c of 20 s, Fig. 21(a) and (b) shows the results obtained with *ESync*, where the estimation error ϵ [as defined in (9)] varies from 5% to 30%. The results returned by Nearest-Job-Next and TSP are also shown for comparison. We can see that *ESync* can tolerate an estimation error as large as 30% when compared with Nearest-Job-Next, and even with 30% estimation error, *ESync* still outperforms TSP by orders of magnitudes.

TABLE III
NUMBER OF PARTIAL AND FULL CHARGES

t_c (s)	20	40	60	80
# of Partial Charges	88.75	77.55	86.00	85.00
# of Full Charges	775.8	702.10	736.60	702.25

6) Impact of the Remaining Energy Threshold: In Section III-A, when the remaining energy levels of sensor nodes are low, the nodes initiate charging requests to the mobile charger. In our aforementioned design, we use the 0% threshold

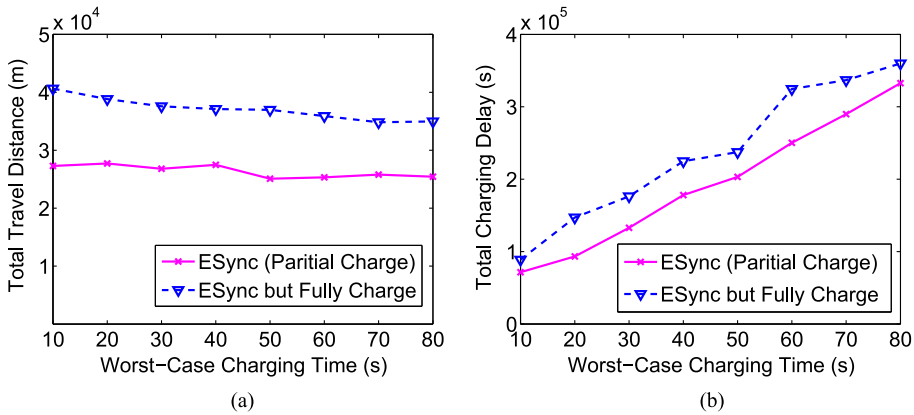

Fig. 23. Advantage of partial charge. (a) Total travel distance. (b) Total charging delay.

only to simplify the presentation (details in the footnote of Section III-A) and, thus, make the charging delay the most straightforward evaluation metric (in which case, the charging delay of sensor nodes is equivalent to their depletion time). It is clear that *ESync* does not require this 0% energy threshold, and in fact, we did have the energy threshold as a control parameter in our simulation. Fig. 11 shows the results obtained with these three methods, where the remaining energy threshold varies from 1% to 6%. Compared with Nearest-Job-Next and TSP, obvious advantages of *ESync* can be observed in all the explored cases.

7) Energy Spatial Randomness: It is intuitive that for multihop sensor networks where the sink is located at the center, *ESync* achieves promising performance because nodes near the sink have higher energy consumption rates. To investigate whether *ESync* performs well in networks without this spatial-correlated energy consumption pattern, we modify the simulation by randomly generating the nodes' energy consumption rates, and the results returned by *ESync*, Nearest-Job-Next, and TSP are shown in Fig. 22(a) and (b). We can see that even when the nodes' energy consumption is irrelevant with their spatial locations, *ESync* still outperforms Nearest-Job-Next and TSP significantly. The advantages of *ESync* over different network scenarios verify its versatility.

8) Ratio of Partial Charging: To facilitate the energy synchronization, sometimes, nodes may be only partially charged. To investigate whether this occasional partial charging of nodes degrades the overall charging performance when compared with always full charging of nodes, we modify *ESync* by making the charger always charge sensor nodes to their full capacity and compare the resultant charging performance with that obtained by the proposed *ESync*. Table III presents the number of partially and fully charged requesting nodes during the simulated charging process. We can see that only around 10% of the requesting nodes are partially charged. To clearly observe the impact of these 10% partially charged requests on the entire charging process, the corresponding charger travel distance and charging delay are shown in Fig. 23(a) and (b), respectively. We can see that although only a small ratio of the requesting nodes is partially charged, they can significantly improve the charging performance when compared with always full charging. Specifically, the charger travel distance and the charging delay of nodes are reduced by around 25% and 20%, respectively. In Fig. 23(a), as shown, the total travel distance is affected by partial charging in *ESync*. The longer charging time itself (in the full-charging case) does not increase the travel distance of the charger, as the charger does not move during that charging time period. However, as the partial charging synchronizes the energy supply of sensor nodes and, thus, reduces the charger travel need in the future, the overall travel distance is reduced when compared with always fully charging nodes.

TABLE IV
AVERAGE INACTIVE RATIO OF NODES

Time to Fully Charge t_c (s)	**20**	**40**	**60**	**80**
ESync	0.0018	0.0030	0.0059	0.0084
NJN	0.0045	0.0088	0.0189	0.0364
TSP	0.4872	0.4869	0.4935	0.4893

9) Average Inactive Ratio of Nodes: To further investigate the performance of *ESync*, we include more evaluation results to shed light on the energy depletion during the mobile charging process. One tricky part is that it is hard to use the number of expired nodes as the evaluation metric, because depleted nodes will be eventually charged by the charger and, thus, resume their operation. As an alternative, we use the average inactive ratio of nodes, which is defined as the ratio between the accumulated inactive time and the total simulated time period, as the evaluation metric. A smaller value of the average inactive ratio of nodes indicates a smaller probability of energy depletion during the mobile charging process; hence, a better performance can be obtained. The results are listed in Table IV. We can see in Table IV that during the time to fully charge t_c varying from 20 to 80 s, *ESync* can always outperform Nearest-Job-Next and TSP significantly. Hence, *ESync* can obtain a better performance to reduce the average energy depletion duration during the mobile charging process.

IX. CONCLUSION

In this paper, we have proposed *ESync*, which is a novel mobile charging protocol for rechargeable sensor networks. Observing the inefficiency of the classic TSP-based mobile charging solutions, we have proposed a *power-*α clustering algorithm to cluster nodes based on their energy consumption rates, and then, a set of nested optimal TSP tours has been constructed

accordingly. A tour selection algorithm has been presented accordingly. As a result, only energy-hungry nodes are involved in the selected TSP tour in each charging round, and thus, the charger travel distance is reduced. Furthermore, we proactively adjust the request sequence of sensor nodes to synchronize it with the selected TSP tour in each charging round, which reduces the charging delay of sensor nodes. The efficiency of *ESync* is verified through both experiments and simulations.

REFERENCES

[1] L. He *et al.*, "ESync: An energy synchronized charging protocol for rechargeable wireless sensor networks," in *Proc. MobiHoc*, 2014, pp. 247–256.

[2] M. Dong *et al.*, "Mobile agent-based energy-aware and user-centric data collection in wireless sensor networks," *Comput. Netw.*, vol. 74, pp. 58–70, Dec. 2014.

[3] S. He *et al.*, "Energy provisioning in wireless rechargeable sensor networks," in *Proc. IEEE INFOCOM*, 2011, pp. 2006–2014.

[4] Y. Li, L. Fu, M. Chen, K. Chi, and Y. Zhu, "RF-based charger placement for duty cycle guarantee in battery-free sensor networks," *IEEE Commun. Lett.*, vol. 19, no. 10, pp. 1802–1805, Aug. 2015.

[5] L. Fu, P. Cheng, Y. Gu, J. Chen, and T. He, "Minimizing charging delay in wireless rechargeable sensor networks," in *Proc. IEEE INFOCOM*, 2013, pp. 2922–2930.

[6] S. He *et al.*, "Energy provisioning in wireless rechargeable sensor networks," *IEEE Trans. Mobile Comput.*, vol. 12, no. 10, pp. 1931–1942, Oct. 2013.

[7] A. Kurs *et al.*, "Wireless power transfer via strongly coupled magnetic resonances," *Science*, vol. 317, no. 5834, pp. 83–86, Jul. 2007.

[8] L. He, L. Kong, Y. Gu, J. Pan, and T. Zhu, "Evaluating the on-demand mobile charging in wireless sensor networks," *IEEE Trans. Mobile Comput.*, vol. 14, no. 9, pp. 1861–1875, Sep. 2015.

[9] Z. Wang, J. Liao, Q. Cao, and H. Qi, "Achieving k-barrier coverage in hybrid directional sensor networks," *IEEE Trans. Mobile Comput.*, vol. 13, no. 7, pp. 1443–1455, Jul. 2014.

[10] A. Abdulla, H. Nishiyama, J. Yang, N. Ansari, and N. Kato, "HYMN: A novel hybrid multi-hop routing algorithm to improve the longevity of WSNs," *IEEE Trans. Wireless Commun.*, vol. 11, no. 7, pp. 2531–2541, Jul. 2012.

[11] Z. Zheng, A. Liu, L. Cai, Z. Chen, and X. Shen, "Energy and memory efficient clone detection in wireless sensor networks," *IEEE Trans. Mobile Comput.*, vol. 15, no. 5, pp. 1130–1143, May 2016.

[12] Q. Zhang *et al.*, "Collaborative scheduling in dynamic environments using error inference," *IEEE Trans. Parallel Distrib. Syst.*, vol. 25, no. 3, pp. 591–601, Mar. 2014.

[13] S. He, J. Chen, X. Li, X. Shen, and Y. Sun, "Mobility and intruder prior information improving the barrier coverage of sparse sensor networks," *IEEE Trans. Mobile Comput.*, vol. 13, no. 6, pp. 1268–1282, Jun. 2014.

[14] Z. Li, Y. Peng, W. Zhang, and D. Qiao, "J-RoC: A joint routing and charging scheme to prolong sensor network lifetime," in *Proc. ICNP*, 2011, pp. 373–382.

[15] Y. Peng, Z. Li, W. Zhang, and D. Qiao, "Prolonging sensor network lifetime through wireless charging," in *Proc. IEEE 31st RTSS*, 2010, pp. 129–139.

[16] S. Zhang, J. Wu, and S. Lu, "Collaborative mobile charging," *IEEE Trans. Comput.*, vol. 64, no. 3, pp. 654–667, Mar. 2014.

[17] Y. Shi, L. Xie, Y. T. Hou, and H. D. Sherali, "On renewable sensor networks with wireless energy transfer," in *Proc. IEEE INFOCOM*, 2011, pp. 1350–1358.

[18] S. Guo, C. Wang, and Y. Yang, "Joint mobile data gathering and energy provisioning in wireless rechargeable sensor networks," *IEEE Trans. Mobile Comput.*, vol. 13, no. 12, pp. 2836–2852, Dec. 2014.

[19] L. He *et al.*, "Mobile-to-mobile energy replenishment in mission-critical robotic sensor networks," in *Proc. IEEE INFOCOM*, 2014, pp. 1195–1203.

[20] L. Fu, P. Cheng, Y. Gu, J. Chen, and T. He, "The optimal charging in wireless rechargeable sensor networks," *IEEE Trans. Veh. Technol.*, vol. 65, no. 1, pp. 278–291, Jan. 2016.

[21] C. Park and P. Chou, "AmbiMax: Autonomous energy harvesting platform for multi-supply wireless sensor nodes," in *Proc. IEEE SECON*, 2006, pp. 168–177.

[22] M. Gorlatova *et al.*, "Challenge: Ultra-low-power energy-harvesting active networked tags (EnHANTs)," in *Proc. MOBICOM*, 2009, pp. 253–260.

[23] A. Kansal, J. Hsu, S. Zahedi, and M. Srivastava, "Power management in energy harvesting sensor networks," *ACM Trans. Embedded Comput. Syst.*, vol. 6, no. 4, pp. 1–38, Sep. 2007.

[24] T. Zhu, Z. Zhong, Y. Gu, T. He, and Z. Zhang, "Leakage-aware energy synchronization for wireless sensor networks," in *Proc. MOBISYS*, 2009, pp. 319–332.

[25] T. Zhu, Y. Gu, T. He, and Z. Zhang, "eShare: A capacitor-driven energy storage and sharing network for long-term operation," in *Proc. SENSYS*, 2010, pp. 239–252.

[26] Y. Shu *et al.*, "Near-optimal velocity control for mobile charging in wireless rechargeable sensor networks," *IEEE Trans. Mobile Comput.*, vol. 15, no. 7, pp. 1699–1713, Jul. 2016.

[27] B. Tong, Z. Li, G. Wang, and W. Zhang, "How wireless power charging technology affects sensor network deployment and routing," in *Proc. IEEE 30th ICDCS*, 2010, pp. 438–447.

[28] M. Zhao, J. Li, and Y. Yang, "Joint mobile energy replenishment and data gathering in wireless rechargeable sensor networks," in *Proc. ITC*, 2011, pp. 238–245.

[29] H. Dai, Y. Liu, G. Chen, X. Wu, and T. He, "SCAPE: Safe charging with adjustable power," in *Proc. IEEE Conf. Comput. Commun. Workshops*, 2014, pp. 203–204.

[30] Y. Zhang, S. He, J. Chen, Y. Sun, and X. Shen, "Distributed sampling rate control for rechargeable sensor nodes with limited battery capacity," *IEEE Trans. Wireless Commun.*, vol. 12, no. 6, pp. 3096–3106, Jun. 2013.

[31] E. Altman and H. Levy, "Queueing in space," *Adv. Appl. Probab.*, vol. 26, no. 4, pp. 1095–1116, Dec. 1994.

[32] J. Bertsimas and G. Van Ryzins, "A stochastic and dynamic vehicle routing problem in the Euclidean plane," *Oper. Res.*, vol. 39, no. 4, pp. 601–615, Jul./Aug. 1991.

[33] Supercapacitors. [Online]. Available: http://batteryuniversity.com

[34] B. P. Wells, "Series resonant inductive charging circuit," U. S. Patent 6 972 543, Aug. 21, 2005.

[35] A. Noda and H. Shinoda, "Selective wireless power transmission through high-flat waveguide-ring resonator on 2-D waveguide sheet," *IEEE Trans. Microw. Theory Techn.*, vol. 59, no. 8, pp. 2158–2167, Aug. 2011.

[36] M. C. Silverman, D. Nies, B. Jung, and G. S. Sukhatme, "Staying alive: A docking station for autonomous robot recharging," in *Proc. IEEE ICRA*, 2002, pp. 1050–1055.

[37] Roomba. [Online]. Available: http://www.irobot.com/

[38] Nokia Wireless Charging Plate. [Online]. Available: http://www.nokia.com/global/products/accessory/dt-900/

[39] Wireless Charging of Electric Bus in Gumi. [Online]. Available: http://kojects.com/2013/08/13/wireless-charging-electric-bus-in-gumi

[40] X. Liu, H. Zhao, X. Yang, X. Li, and N. Wang, "Trailing mobile sinks: A proactive data reporting protocol for wireless sensor networks," in *Proc. IEEE 7th MASS*, 2010, pp. 214–223.

[41] V. Kulathumani, A. Arora, M. Sridharan, and M. Demirbas, "Trail: A distance-sensitive sensor network service for distributed object tracking," *ACM Trans. Sens. Netw.*, vol. 5, no. 2, pp. 1–40, 2009.

[42] G. Xing, T. Wang, W. Jia, and M. Li, "Rendezvous design algorithms for wireless sensor networks with a mobile base station," in *Proc. MobiHoc*, 2008, pp. 231–240.

[43] Intel Berkeley Res. Lab. Data. [Online]. Available: http://www.select.cs.cmu.edu/data/labapp3/index.html

[44] Concorde TSP Solder. [Online]. Available: http://www.tsp.gatech.edu/concorde.html

[45] Y. Wang, M. C. Vuran, and S. Goddard, "Stochastic analysis of energy consumption in wireless sensor networks," in *Proc. IEEE SECON*, 2010, pp. 1–9.

[46] X. Jiang, P. Dutta, D. Culler, and I. Stoica, "Micro power meter for energy monitoring of wireless sensor networks at scale," in *Proc. IPSN*, 2007, pp. 186–195.

[47] V. Shnayder, M. Hempstead, B. Rong Chen, G. W. Allen, and M. Welsh, "Simulating the power consumption of large-scale sensor network applications," in *Proc. SENSYS*, 2004, pp. 188–200.

[48] C. Wang, J. Li, F. Ye, and Y. Yang, "NETWRAP: An NDN based real-timewireless recharging framework for wireless sensor networks," *IEEE Trans. Mobile Comput.*, vol. 13, no. 6, pp. 1283–1297, Jun. 2014.

[49] J. Beardwood, J. Halton, and J. Hammersley, "The shortest path through many points," *Math. Proc. Cambridge Philosoph. Soc.*, vol. 55, no. 2, pp. 145–148, Apr. 1959.

[50] C. Wang, J. Li, F. Ye, and Y. Yang, "Recharging schedules for wireless sensor networks with vehicle movement costs and capacity constraints," in *Proc. IEEE SECON*, 2014, pp. 468–476.

[51] L. Oakes *et al.*, "Surface engineered porous silicon for stable, high performance electrochemical supercapacitors," *Sci. Rep.*, vol. 3, no. 3020, pp. 1–7, Oct. 2013.
[52] NCR18650. [Online]. Available: http://www.panasonic.com
[53] Elixir II. [Online]. Available: https://play.google.com/store/apps/
[54] O. Gnawali, R. Fonseca, K. Jamieson, D. Moss, and P. Levis, "Collection tree protocol," in *Proc. SenSys*, 2009, pp. 1–14.
[55] Y. Zhang, S. He, and J. Chen, "Data gathering optimization by dynamic sensing and routing in rechargeable sensor networks," *ACM/IEEE Trans. Netw.*, vol. 24, no. 3, pp. 1632–1646, Jul. 2016.

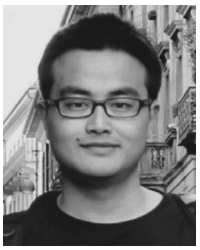

Lingkun Fu (S'13–M'15) is currently working toward the Ph.D. degree with the Group of Networked Sensing and Control (IIPC-NesC), State Key Laboratory of Industrial Control Technology, Zhejiang University, Hangzhou, China.

His research interests include optimization for wireless rechargeable sensor networks, mobile computing, and cyberphysical systems.

Liang He (S'09–M'12) received the B.Eng. degree from Tianjin University, Tianjin, China, in 2006 and the Ph.D. degree from Nankai University, Tianjin, in 2011.

He is currently a Research Fellow with the University of Michigan, Ann Arbor, MI, USA. He was a Research Scientist with Singapore University of Technology, Singapore, during 2011–2014 and a Research Assistant with the University of Victoria, Victoria, BC, Canada, during 2009–2011.

Dr. He received Best Paper Awards at the 2011 IEEE International Conference on Wireless Communications and Signal Processing, the 2011 IEEE Global Telecommunications Conference (GLOBECOM), and the 2015 International Conference on Heterogeneous Networking for Quality, Reliability, Service and Robustness (QShine). He was also a candidate for the Best Paper Award at 2014 IEEE GLOBECOM.

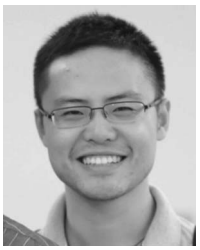

Peng Cheng (M'10) received the B.E. degree in automation and the Ph.D. degree in control science and engineering from Zhejiang University, Hangzhou, China, in 2004 and 2009, respectively.

He is currently an Associate Professor with the Department of Control Science and Engineering, Zhejiang University. His research interests include networked sensing and control, cyberphysical systems, and robust control.

Dr. Cheng serves as an Associate Editor for *Wireless Networks* and the *International Journal of Communication Systems*. He also served as a Publicity Cochair for the 2013 IEEE International Conference on Mobile Ad hoc and Sensor Systems and a Local Arrangement Chair for the 2015 ACM International Symposium on Mobile Ad Hoc Networking and Computing.

Yu Gu (M'10) received the Ph.D. degree from the University of Minnesota Twin Cities, Minneapolis, MN, USA, in 2010.

He is currently a Research Scientist for Watson Health Cloud with IBM Watson Health, Cambridge, MA, USA. From 2010 to 2014, he was an Assistant Professor with Singapore University of Technology and Design, Singapore. He is an author and a coauthor of over 100 papers in premier journals and conferences. His publications have been selected as graduate-level course materials by over 20 universities in the United States and other countries. His research interests include networked embedded systems, wireless sensor networks, cyberphysical systems, wireless networking, real-time and embedded systems, distributed systems, vehicular ad hoc networks, and stream computing systems.

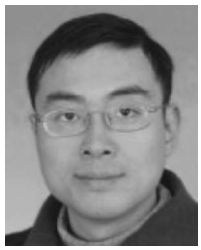

Jianping Pan (S'96–M'98–SM'08) received the Bachelor's and Ph.D. degrees in computer science from Southeast University, Nanjing, China.

He is currently a Professor with the Department of Computer Science, University of Victoria, Victoria, BC, Canada. He was a Postdoctoral Researcher with the University of Waterloo, Waterloo, ON, Canada. He was also with Fujitsu Labs and NTT Labs. His area of specialization is computer networks and distributed systems, and his current research interests include protocols for advanced networking, performance analysis of networked systems, and applied network security.

Dr. Pan received Best Paper Awards from the 2009 Institute of Electronics, Information, and Communications Engineers Conference; the 2011 IEEE International Conference on Wireless Communications and Signal Processing; the 2011 IEEE Global Telecommunications Conference; and the 2013 IEEE International Conference on Communications. He also received the Telecommunications Advancement Foundation's Telesys Award in 2010 and the Japan Society for the Promotion of Science Invitation Fellowship in 2012.

Jiming Chen (M'08–SM'11) received the B.Sc. and Ph.D. degrees in control science and engineering from Zhejiang University, Hangzhou, China, in 2000 and 2005, respectively.

He was a Visiting Researcher with the French Institute for Research in Computer Science and Automation (INRIA), Rocquencourt, France, in 2006; the National University of Singapore, Singapore, in 2007; and the University of Waterloo, Waterloo, ON, Canada, from 2008 to 2010. He is currently a Full Professor with the Department of Control Science and Engineering; the coordinator of the Networked Sensing and Control Group, State Key Laboratory of Industrial Control Technology; and the Vice Director of the Institute of Industrial Process Control, Zhejiang University.

Dr. Chen currently serves as an Associate Editor for several international journals, including the IEEE TRANSACTIONS ON PARALLEL AND DISTRIBUTED SYSTEMS, the IEEE TRANSACTIONS ON INDUSTRIAL ELECTRONICS, the IEEE TRANSACTIONS ON INDUSTRIAL INFORMATICS, IEEE NETWORK, and the IEEE TRANSACTIONS ON CONTROL OF NETWORK SYSTEMS. He was a Guest Editor of the IEEE TRANSACTIONS ON AUTOMATIC CONTROL, *Computer Communication* (Elsevier), *Wireless Communication and Mobile Computer* (Wiley), and the *Journal of Network and Computer Applications* (Elsevier).